Scientia Africana, Vol. 17 (No. 1), June 2018. Pp 89-102
© Faculty of Science, University of Port Harcourt, Printed in Nigeria *ISSN 1118 – 1931*

EFFECTS OF VARIABLE THERMAL CONDUCTIVITY ON RADIATIVE MHD FLOW IN A POROUS MEDIUM BETWEEN TWO VERTICAL WAVY WALLS

[1]A. B. Disu and M. S. Dada[2]

[1]Department of Mathematics, National Open University of Nigeria, Abuja, Nigeria
adisu@noun.edu.ng
[2]Department of Mathematics, University of Ilorin, Ilorin, Nigeria.
msadada@unilroin.edu.ng

Received: 03-04-18
Accepted:23-04-18

ABSTRACT

An analysis was carried out on the effects of variable thermal conductivity on radiative MHD flow in a porous medium between two vertical wavy walls. The thermal conductivity is assumed a linear function of temperature and the fluid flow consists of two parts namely a mean and perturbed part, where the perturbed component is expressed as complex exponential series in terms of short wave length. The resultant governing equations were solved using Homotopy Analysis Method (HAM). The effects of the fluid parameters characterizing the velocity, temperature, fluid pressure, skin friction and Nusselt number were analysed and discussed.

Key words: A porous medium; Homotopy analysis method; Radiative MHD flow; Variable thermal conductivity; Wavy walls.

INTRODUCTION

Considerable attention of researchers has been drawn to the study of an incompressible viscous fluid flow between wavy wall(s) in the last few decades. This is due to its applications in engineering and industry such as in design cooling system for electronic components, design of ventilation for heating buildings and design of storage facilities for agricultural produce. The wavy channel is often used for MHD flow in many applications such as crude oil refinement, glass manufacturing and paper production (Akbar, 2015).

The importance of flow in wavy wall(s) led Fasogbon (2006) to investigate the effects of magnetic field on the viscous incompressible fluid in corrugated channel. The author reported that the magnetic field slow down the fluid velocity. Heat transfer with radiation in the MHD free convection between a vertical wavy wall and a parallel flat wall was studied by Tak and Kumar (2007). The authors concluded the thermal radiation has an accelerating effect on the velocity and temperature profiles. Fasogbon (2010) presented heat and mass transfer by free convection in an irregular channel. The investigator reported that the effects of different chemical species on the fluid flow. The heat transfer of viscous incompressible fluid with slip effects within a spirally enhanced channel was studied by Abubakar (2014) and concluded that the slip effects increase the fluid velocity. In the aforementioned studies, the investigations were narrowed down to one vertical wavy with a parallel flat wall.

Tak and Kumar (2006) and Kumar (2011) studied the viscous incompressible fluid in a

two-dimensional vertical wavy channel and highlighted that radiation increases the fluid flow while heat source reduces the fluid flow in a non-Darcy porous medium.

The study of fluid flow through a porous medium has vital applications in heat removal from nuclear fuel debris, underground disposal of radiative waste material and storage of food stuffs. Above mentioned applications of porous media led Teneja and Jain (2004) to analyse the MHD free convection flow in the presence of temperature dependent heat source in a viscous incompressible fluid confined between a long vertical wavy wall and a parallel flat wall in slip flow regime with constant heat flux. Heat transfer with radiation and temperature heat source in a porous medium between two vertical wavy walls studied by Dada and Disu (2015). The authors reported that the velocity of the fluid increases with the increase in the permeability of the porous medium. Disu and Dada (2017) studied Reynolds' model viscosity on radiative MHD flow in a porous medium between two vertical wavy walls. The authors observed that an increase in variable viscosity parameter increases the velocity of the fluid.

The thermal conductivity of the fluid flow in all the above studies is assumed constant throughout the flow regime. However, it is a known fact that the thermal conductivity changes with temperature within the fluid flow. For example, the thermal conductivity of engine oil at 20^0C and 80^0C are 0.145W/mK and 0.138 W/mK respectively. Some studies of variable thermal conductivity of the fluid flow over a stretching sheet, parallel walls and pipe have been reported (Chaim, 1992; Sharma and Singh, 2009).

In view of the above, it is necessary to extend the variation of the thermal conductivity to the study of the fluid flow in a porous medium between two vertical wavy walls. Therefore, we present the effects of variable thermal conductivity on MHD radiative flow in a porous medium between two vertical wavy walls. Thermal conductivity is assumed a linear function of temperature and Darcy model is used for porous medium.

Formulation of the problem

Consider a two-dimensional free convective, steady laminar and hydromagnetic-radiative flow in a Darcy's model porous medium between two vertical wavy walls (Figure 1). The X-axis is taken vertically upwards and Y -axis perpendicular to it. The wavy walls are represented by $Y = \varepsilon^* \cos(\Lambda X)$ and $Y = L + \varepsilon^* \cos(\Lambda X)$ respectively, where $\varepsilon^* \ll 1$. The fluid flow takes place under buoyancy and temperature dependent heat. The governing equations of the fluid flow and heat transfer are given below:

Scientia Africana, Vol. 17 (No. 1), June 2018. Pp 89-102
© Faculty of Science, University of Port Harcourt, Printed in Nigeria *ISSN 1118 - 1931*

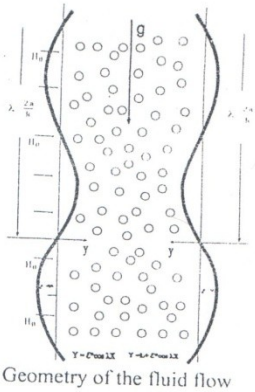

Figure 1: Geometry of the fluid flow

$$\frac{\partial U}{\partial X}+\frac{\partial V}{\partial Y}=0, \tag{1}$$

$$\rho\left(U\frac{\partial U}{\partial X}+V\frac{\partial U}{\partial Y}\right)=-\frac{\partial P}{\partial X}+\mu\left(\frac{\partial^2 U}{\partial X^2}+\frac{\partial^2 U}{\partial Y^2}\right)+g\beta(T-T_L)-H_0^2U-\frac{\mu}{K^*}U, \tag{2}$$

$$\rho\left(U\frac{\partial V}{\partial X}+V\frac{\partial V}{\partial Y}\right)=-\frac{\partial P}{\partial Y}+\mu\left(\frac{\partial^2 V}{\partial X^2}+\frac{\partial^2 V}{\partial Y^2}\right)-\frac{\mu(T)}{K^*}U, \tag{3}$$

$$\rho C_P\left(U\frac{\partial T}{\partial X}+V\frac{\partial T}{\partial Y}\right)=\frac{\partial}{\partial X}\left(k(T)\frac{\partial U}{\partial X}\right)+\frac{\partial}{\partial Y}\left(k(T)\frac{\partial U}{\partial Y}\right)-\frac{\partial q_x}{\partial X}-\frac{\partial q_y}{\partial Y}+Q(T_L-T). \tag{4}$$

The boundary conditions are taken as:

$$U=0, V=0, T=T_C \text{ at } Y=\varepsilon^*\cos(\Lambda X),$$
$$U=0, V=0, \frac{\partial T}{\partial Y}=0 \text{ at } Y=L+\varepsilon^*\cos(\Lambda X), \tag{5}$$

where U, V are the velocity components in X and Y directions, P is the fluid pressure, μ is the dynamics viscosity, g is the acceleration due to gravity, β is the coefficient of volume expansion, T is the fluid temperature, H_0 is the uniform magnetic field, K^* is the porosity parameter, $k(T)$ is the variable thermal conductivity, ρ is the density of the fluid, C_P is the specific heat at constant pressure, Q is the heat source, T_L is the equilibrium temperature, q_x is the radiative heat flux in the X −direction and q_y is the radiative heat flux in the Y −direction.

The Rosseland approximation defined the radiative heat flux in the X and Y directions as Brewster (1972)

$$q_x=\frac{4\sigma}{3R_1}\left(\frac{\partial T^4}{\partial X}\right),\quad q_y=\frac{4\sigma}{3R_1}\left(\frac{\partial T^4}{\partial y}\right), \tag{6}$$

where R_1 is the mean absorption coefficient and σ is the Stefan-Boltzmann constant. Assuming the temperature differences within the fluid flow are sufficiently small such that T^4 may be expressed as a linear function of the temperature, then the Taylor series expansion of T^4 about T_L, after neglecting higher order terms, is given by

$$T^4 = 4T_L^3 T - 3T_L^4. \quad (7)$$

The thermal conductivity is assumed to vary as a linear function of temperature (Slattery (1972); Sharma and Singh (2009))

$$k(T) = k[1 + d(T - T_L)]. \quad (8)$$

The non-dimensional parameters are defined as

$$x = \frac{X}{L}, y = \frac{Y}{L}, u = \frac{LU}{\nu}, v = \frac{LV}{\nu}, p = \frac{PL^2}{\rho\nu^2}, S = d(T_0 - T_L), \theta = \frac{T-T_L}{T_0-T_L}, Pr = \frac{\mu C_p}{k}, G = \frac{bg\beta L^2}{\rho\upsilon}, R = \frac{k a_R}{4\delta T_\infty^3}, \alpha = \frac{QL^2}{k}, M = \frac{H_0 L^2}{\rho\upsilon}, K = \frac{K^*}{\upsilon L^2}, \lambda = \Lambda L, \ \varepsilon = \frac{\varepsilon^*}{L} \quad (9)$$

S is the thermal conductivity variation parameter, Pr is the Prandtl, G is the Grasshof number, R is radiation parameter, α is the heat source parameter, M is the magnetic parameter, K is the porosity parameter, λ is the dimensionless frequency and ε is the dimensionless amplitude ratio.

Using Eq. (9), Eq. (8) becomes

$$k(T) = k[1 + S\theta]. \quad (10)$$

Then, Eqs. (1) - (4) are in non-dimensional form as

$$\frac{\partial u}{\partial x} + \frac{\partial v}{\partial y} = 0 \quad (11)$$

$$u\frac{\partial u}{\partial x} + v\frac{\partial u}{\partial y} = -\frac{\partial p}{\partial x} + \frac{\partial^2 u}{\partial x^2} + \frac{\partial^2 u}{\partial y^2} + G\theta - Mu - \frac{1}{K}u, \quad (12)$$

$$u\frac{\partial v}{\partial x} + v\frac{\partial v}{\partial y} = -\frac{\partial p}{\partial y} + \frac{\partial^2 u}{\partial x^2} + \frac{\partial^2 v}{\partial y^2} + \frac{1}{K}v, \quad (13)$$

$$\left(u\frac{\partial \theta}{\partial x} + v\frac{\partial \theta}{\partial y}\right) = \left(\frac{\partial^2 \theta}{\partial x^2} + \frac{\partial^2 \theta}{\partial y^2}\right) + S\left(\frac{\partial \theta}{\partial x}\right)^2 + S\left(\frac{\partial \theta}{\partial y}\right)^2 - \alpha\theta, \quad (14)$$

with the boundary conditions:

$$u = 0, v = 0, \theta = 1 \text{ at } y = \varepsilon\cos(\lambda x),$$
$$u = 0, v = 0, \frac{\partial \theta}{\partial y} = 1 \text{ at } y = 1 + \varepsilon\cos(\lambda x), \quad (15)$$

where $\omega = \left(1 + \frac{4}{3R}\right)$ is the radiation parameter.

We assume that the solution consists of a mean part and a perturbed part so that the velocity and temperature distributions are

$$\left.\begin{aligned} u(x,y) &= u_0(y) + \varepsilon u_1(x,y) \\ v(x,y) &= \varepsilon v_1(x,y) \\ P(x,y) &= P_0(x) + \varepsilon p_1(x,y) \\ \theta(x,y) &= \theta_0(y) + \varepsilon\theta_1(x,y) \end{aligned}\right\}. \quad (16)$$

Substituting Eq. (16) into Eqs. (11) - (14) with boundary conditions (15), we obtain the following set of equations:

zeroth order equations are

$$\frac{d^2u_0}{dy^2} - Mu_0 - \frac{1}{K}u_0 + G\theta_0 = C, \quad (17)$$

$$(\omega + S\theta_0)\frac{d^2\theta_0}{dy^2} + S\left(\frac{d\theta_0}{dy}\right)^2 - \alpha\theta_0 = 0, \quad (18)$$

where $C = \frac{du_0}{dy}$,

with boundary conditions

$$\left.\begin{aligned} u_0 &= 0, & \theta_0 &= 1, & y &= 0 \\ u_0 &= 0, & \frac{d\theta_0}{dy} &= 0, & y &= 1 \end{aligned}\right\}. \quad (19)$$

First order equations are

$$\frac{\partial u_1}{\partial x} + \frac{\partial v_1}{\partial y} = 0 \quad (20)$$

$$u_0\frac{\partial u_1}{\partial x} + v_1\frac{du_0}{dy} = -\frac{\partial p_1}{\partial x} + \frac{\partial^2 u_1}{\partial x^2} + \frac{\partial^2 u_1}{\partial y^2} + G\theta_1 - Mu_1 - \frac{1}{K}u_1, \quad (21)$$

$$u_0\frac{\partial u_1}{\partial x} = -\frac{\partial p_1}{\partial y} + \frac{\partial^2 v_1}{\partial x^2} + \frac{\partial^2 v_1}{\partial y^2} - \frac{1}{K}v_1, \quad (22)$$

$$Pr\left(u_0\frac{\partial \theta_1}{\partial x} + v_1\frac{d\theta_0}{dy}\right) = \omega\left(\frac{\partial^2 \theta_1}{\partial x^2} + \frac{\partial^2 \theta_1}{\partial y^2}\right) + 2S\left(\frac{d\theta_0}{dy}\frac{\partial \theta_1}{\partial y}\right) - \alpha\theta_1, \quad (23)$$

with boundary conditions

Scientia Africana, Vol. 17 (No. 1), June 2018. Pp 89-102
© Faculty of Science, University of Port Harcourt, Printed in Nigeria *ISSN 1118 – 1931*

$$\left.\begin{array}{ll} u_1 = -\frac{du_0}{dy}, \quad v_1 = 0, \ \theta_1 = -\frac{d\theta_0}{dy} & y = 0 \\ u_1 = 0, \quad v_1 = 0, \ \frac{d\theta_1}{dy} = 0, & y = 1 \end{array}\right\}. \quad (24)$$

Eqs. (20) – (23) with boundary conditions (24) are simplified by introducing the stream function $\psi(x, y)$such that

$$u_1 = -\frac{d\psi}{dy}, \ v_1 = \frac{d\psi}{dx} \quad (25)$$

Therefore, Eqs. (20) - (23) and boundary conditions (24) becomes

$$u_0\left(\frac{\partial^3\psi}{\partial x^3} + \frac{\partial^3\psi}{\partial x \partial y^2}\right) - \frac{d^2u_0}{dy^2}\frac{\partial\psi}{\partial x} - \frac{\partial^4\psi}{\partial x^4} - \frac{\partial^4\psi}{\partial y^4} - 2\frac{\partial^4\psi}{\partial x^2\partial y^2} + M\frac{\partial^2\psi}{\partial y^2} + \frac{1}{K}\frac{\partial^2\psi}{\partial y^2} + G\frac{d\theta_1}{dy} = 0, \quad (26)$$

$$Pr\left(u_0\frac{\partial\theta_1}{\partial x} + \frac{\partial\psi}{\partial x}\frac{d\theta_0}{dy}\right) = \omega\left(\frac{\partial^2\theta_1}{\partial x^2} + \frac{\partial^2\theta_1}{\partial y^2}\right) + 2S\left(\frac{d\theta_0}{dy}\frac{\partial\theta_1}{\partial y}\right) - \alpha\theta_1, \quad (27)$$

with boundary conditions

$$\left.\begin{array}{ll} \frac{\partial\psi}{\partial y} = -\frac{du_0}{dy}, \ \frac{\partial\psi}{\partial x} = 0, \ \theta_1 = -\frac{d\theta_0}{dy} & y = 0 \\ \frac{\partial\psi}{\partial y} = 0, \ \frac{\partial\psi}{\partial x} = 0, \ \frac{d\theta_1}{dy} = 0, & y = 1 \end{array}\right\}. \quad (28)$$

Due to the nature of the wall motion, we assume wave-like solutions of the form

$$\psi(x, y) = Re\left(\sum_r \psi_r \lambda^r e^{i\lambda x}\right) \quad (29)$$

$$\theta_1(x, y) = Re\left(\sum_r t_r \lambda^r e^{i\lambda x}\right) \quad (30)$$

where $r = 0, 1$.

Substituting Eqs. (29) and (30) into Eqs. (26) and (27) with boundary conditions (28), the sets of obtained equations are:

$$\frac{d^4\psi_0}{dy^4} - M\frac{d^2\psi_0}{dy^2} + \frac{1}{K}\frac{d^2\psi_0}{dy^2} - G\frac{dt_0}{dy} = 0, \quad (31)$$

$$(\omega + S\theta_0)\frac{d^2t_0}{dy^2} + 2S\left(\frac{d\theta_0}{dy}\frac{dt_0}{dy}\right) - \alpha t_0 = 0, \quad (32)$$

with the boundary conditions

$$\left.\begin{array}{ll} \frac{d\psi_0}{dy} = -\frac{du_0}{dy}, \ \psi_0 = 0, \ t_0 = -\frac{d\theta_0}{dy} & y = 0 \\ \frac{\partial\psi_0}{\partial y} = 0, \ \psi_0 = 0, \ \frac{dt_0}{dy} = 0, & y = 1 \end{array}\right\}. \quad (33)$$

$$\frac{d^4\psi_1}{dy^4} - M\frac{d^2\psi_0}{dy^2} - \frac{1}{K}\frac{d^2\psi_1}{dy^2} + i\left(\psi_0\frac{d^2u_0}{dy^2} - u_0\frac{d^2\psi_0}{dy^2}\right) - G\frac{dt_1}{dy} = 0, \quad (34)$$

$$(\omega + S\theta_0)\frac{d^2t_1}{dy^2} + 2S\frac{d\theta_0}{dy}\frac{dt_1}{dy} - \alpha t_1 = iPr\left(u_0t_0 + \psi_0\frac{d\theta_0}{dy}\right), \quad (35)$$

with the boundary conditions

$$\left.\begin{array}{ll} \frac{d\psi_1}{dy} = 0, \ \psi_1 = 0, \ t_1 = 0 & y = 0 \\ \frac{\partial\psi_1}{\partial y} = 0, \ \psi_1 = 0, \ t_1 = 0, & y = 1 \end{array}\right\}. \quad (36)$$

The Homotopy Analysis Method of Solution

The solution of Eqs. (17) and (18) with condition (19) are obtained by constructing zeroth-order deformation (Liao (2004); Cheng *et al* (2008); Liao (2012)) as

$$(1 - q)L[u_0(y; q) - u_i(y)] = hqH(y)N[u_0(y, q)] \quad (37)$$

$$(1 - q)L[\theta_0(y; q) - \theta_i(y)] = hqH(y)N[\theta_0(y, q)] \quad (38)$$

$$\left.\begin{array}{l} u_0(0; q) = 0, \ u_0(1: q) = 0 \\ \theta_0(0; q) = 0, \ \frac{d\theta_0(1;q)}{dy} = 0, \end{array}\right\} \quad (39)$$

$q \in [0,1]$ is the embedding parameter, L is the auxiliary operator , u_i and θ_i are the initial guesses of unknown function $u_0(y; q)$ and $\theta_0(y; q)$, h is the auxiliary parameter, $H(y) \neq 0$ is the auxiliary function and N is the nonlinear operator.

when $q = 0$ and $q = 1$, the followings are obtained

$$u_0(y; 0) = u_i, \theta_0(y; 0) = \theta_i \quad (40)$$

$$u_0(y; 1) = u_0(y), \theta_0(y; 1) = \theta_0(y) \quad (41)$$

Using the Maclaurin series, $u_0(y;q)$ and $\theta_0(y;q) = u_i$ can be expanded with respect to q

$u_0(y;0) = u_i + \sum_{m=1}^{n} u_{0m}(y)q^m$ (42)

$\theta_0(y;0) = \theta_i + \sum_{m=1}^{n} \theta_{0m}(y)q^m$ (43)

where $u_{0m} = \frac{1}{m!}\frac{\partial^m u_0(y;q)}{\partial q^m}\Big|_{q=0}$ and $\theta_{0m} = \frac{1}{m!}\frac{\partial^m \theta_0(y;q)}{\partial q^m}\Big|_{q=0}$

Assuming the Eqs. (42) and (43) converge at $q = 1$, the equations yield

$u_0(y;0) = u_i + \sum_{m=1}^{n} u_{0m}(y)$ (44)

$\theta_0(y;0) = \theta_i + \sum_{m=1}^{n} \theta_{0m}(y)$ (45)

Eqs. (37) and (38) are differentiated with respect to q m −times, then setting $q = 0$ and divided by $m!$ (Cheng, 2008) and (Liao, 2012). The following m −order deformation equations are obtained

$u_{0m}(y) = \chi_m u_0(m-1) + L^{-1}(hH(y)Ru_{0m})$, (46)

$\theta_{0m}(y) = \chi_m \theta_0(m-1) + L^{-1}(hH(y)R\theta_{0m})$, (47)

where, $\chi_m = \begin{cases} 0, & m \le 1 \\ 1, & m > 2 \end{cases}$ (48)

$Ru_{0m} = u''_{0(m-1)} - Mu_{0m} - \frac{1}{K}u_{0m} + G\theta_{0m}$ (49)

$R\theta_{0m} = \omega\theta''_{0(m-1)} + S\sum_{n=0}^{m-1}\theta_{0m}\theta''_{0(m-1)} + S\sum_{n=0}^{m-1}\theta'_{0m}\theta'_{0(m-1)} - \alpha\theta_{0m}$ (50)

In the similar way, the following equations are obtained for ψ_0, t_0, ψ_1 and t_1 and these are given as follows

$\psi_{0m}(y) = \chi_m\psi_0(m-1) + L^{-1}(hH(y)R\psi_{0m})$, (51)

$t_{0m}(y) = \chi_m t_0(m-1) + L^{-1}(hH(y)Rt_{0m})$, (52)

$\psi_{1m}(y) = \chi_m\psi_1(m-1) + L^{-1}(hH(y)R\psi_{1m})$, (53)

$t_{1m}(y) = \chi_m t_1(m-1) + L^{-1}(hH(y)Rt_{1m})$, (54)

where

$R\psi_{0m} = \psi^{iv}_{0(m-1)} - M\psi''_{0m-1} - \frac{1}{K}\psi''_{0m-1} + Gt'_{0m-1}$ (55)

$Rt_{0m} = \omega t''_{0(m-1)} + S\sum_{n=0}^{m-1}\theta_{0m}t''_{0(m-1)} + S\sum_{n=0}^{m-1}\theta'_{0m}t''_{0(m-1-n)} + 2S\sum_{n=0}^{m-1}\theta'_{0m}t'_{0(m-1-n)} - \alpha t_{0m}$ (56)

$R\psi_{1m} = \psi^{iv}_{1(m-1)} - M\psi''_{1m-1} - \frac{1}{K}\psi''_{0m-1} + Gt'_{1m-1} - i\left(\sum_{n=0}^{m-1}u_{0n}\psi''_{0(m-1-n)} = \sum_{n=0}^{m-1}u_{0n}\psi'_{0(m-1-n)}\right)$ (57)

$Rt_{1m} = \omega t''_{1(m-1)} + S\sum_{n=0}^{m-1}\theta_{1m}t''_{0(m-1)} + S\sum_{n=0}^{m-1}\theta'_{1m}t''_{1(m-1-n)} + 2S\sum_{n=0}^{m-1}\theta'_{1m}t'_{0(m-1-n)} - \alpha t_{0m} - i\left(\sum_{n=0}^{m-1}u_{0n}t_{0m-1-n} + \sum_{n=0}^{m-1}\theta'_m\psi_{0(m-1-n)}\right)$ (58)

Fluid pressure

The fluid pressure $P(X,Y)$ for Eqs. (2) and (3) is defined as

$P(X,Y) = \int dP = \int\left(\frac{\partial P}{\partial X}dX + \frac{\partial P}{\partial Y}dY\right)$.

(59) Using Eqs. (11), (12), (16), (25), (29) and (30) in Eq(59), then Eq. (59) becomes

$p(x,y) = x\left(u''_0 - Mu_0 - \frac{1}{K}u_0 + G\theta_0\right) + Re\left[u_0\psi'_0 - u'_0\psi_0 - \gamma\theta'_0\psi_0 + i\left(\psi'''_1 - +M\psi'_1 + \frac{1}{K}\psi'_1 + Gt_1\right) + \frac{i}{\lambda}\left(\psi'''_0 + M\psi'_0 + \frac{1}{K}\psi'_0 + Gt_0\right) + i\lambda\int\left(\psi''_0 - M\psi_0 + \frac{1}{K}\psi_0\right)dy\right]e^{i\lambda x}$ (60)

Eq. (60) can be expresssed as $\Delta p = p(x,y) - p(x,1)$ where Δp is the pressure drop which is the pressure at point y in the fluid flow with respect to x (Fasogbon (2010)). The pressure drop (Δp) is at 2π or $\lambda x = 0$

Skin Friction

The shear stress at the walls $y = \epsilon\cos(\lambda x)$ and $y = 1 + \epsilon\cos(\lambda x)$ are given as

$\tau = u'(0) + \epsilon\left(-\psi''_r(0)\cos(\lambda x) + \lambda\psi''_i(0)\sin(\lambda x)\right)$ (68)

$\tau = u'(1) + \epsilon\left(-\psi''_r(1)\cos(\lambda x) + \lambda\psi''_i(1)\sin(\lambda x)\right)$ (69)

Scientia Africana, Vol. 17 (No. 1), June 2018. Pp 89-102
© Faculty of Science, University of Port Harcourt, Printed in Nigeria *ISSN 1118 – 1931*

Nusselt Number

The rate of heat transfers at the walls $y = \epsilon\cos(\lambda x)$ and $y = 1 + \epsilon\cos(\lambda x)$

$$Nu = -\theta'(0) - \epsilon\left(-t_r'(0)\cos(\lambda x) + \lambda t_i'(0)\sin(\lambda x)\right) \quad (70)$$

$$Nu = -\theta'(1) - \epsilon\left(-t_r'(0)\cos(\lambda x) + \lambda t_i'(1)\sin(\lambda x)\right) \quad (71)$$

Discussion of Results

Eqs. (49) - (50), (59) - (62) are implemented and solved on Maple 18. The following series of computations are carried out to determine the effects of variable conductivity parameter (S), heat source (α), radiation parameter (ω), magnetic parameter (M), Grashof number (G), permeability parameter (K), frequency (λ), and amplitude (ε), on the velocity, temperature, skin friction as well as Nusselt number. The analysis of the fluid flow and heat transfer distribution profiles were carried out with the following fixed values for the parameters: $S = 0.1,\ M = 1.0, K = 1.0, \alpha = 1.0,\ \omega = 0.1, G = 5.0, \varepsilon = 0.1, \lambda = 0.01$ and $x = 1.0$. All the graphs use the default values expect otherwise stated.

The effect of the magnetic parameter (M) on the velocity profiles is depicted in Figure 2. The presence of the magnetic field normal to the fluid flow in an electrically conducting fluid introduced a Lorentz force which act against the flow. This resistive force slow down the the flow and hence the fluid velocity decreases with increase of magnetic field parameter. Figure 3 presents the variation of velocity profiles with permeability parameter. It is observed that the presence of permeability parameter reduces the resistance of the porous medium thereby enhance the fluid velocity. Figure 4 depicts the variation of velocity distribution with different value of Grashof number. It can be seen that an increase in Grashof number leads to a rise in velocity profiles. Figure 5 illustrates the effects of variable thermal conductivity on the velocity profiles. It is noted that as S increase (as thermal conductivity increases with temperature), the velocity increases.

Figures 6 and 7 represent the influence of heat source (α) and thermal radiation parameter (ω) respectively on the velocity profiles. It is observed that an increase in heat source parameter causes a reduction in the buoyancy effect which reduces the fluid velocity. It can be seen that the velocity profile increases as the radiation parameter (ω) increases, thereby increasing the momentum boundary layer thickness. This is because the intensity of heat produced through thermal radiation increases thereby breaking the bond holding the components of the fluid particles together and as the fluid velocity increases.

Figure 8 shows the temperature profiles for different values of thermal conductivity parameter(S). It can be seen that an increase in thermal conductivity parameter increases the temperature profiles. Figure 9 illustrates the influence of heat source parameter (α) on temperature profiles. It is observed that the temperature of the fluid decreases with an increase in the values of the heat source. The variation of temperature profiles for different values of thermal radiation parameter (ω) is shown in Figure 10. The results show that the temperature profile increase in the thermal radiation parameter and hence increasing the thermal boundary layer thickness

Figure 11 depicts the fluid pressure with different values of magnetic parameter(M). It is observed that an increase in magnetic parameter decreases the fluid pressure

profile. Figure 12 represents the variation of permeability parameter on the fluid pressure. It is observed that an increase in the permeability parameter causes a reduction in the fluid pressure. It can be seen that the fluid pressure increases with an increase in the Grashof parameter in Figure 13. Figure 14 illustrates the influence of thermal radiation parameter (ω) on the fluid pressure. It can be noticed that fluid pressure decreases as the radiation parameter increases. Figure 15 presents the trend of the fluid pressure with variation of heat source parameter(α). It can be seen that an increase in heat source parameter produces a rise in the fluid pressure. Figure 16 represents the variation of thermal conductivity parameter (S) on the fluid pressure profiles. It is observed that an increase in thermal conductivity increases the fluid pressure profiles.

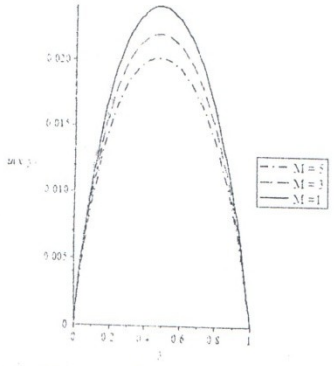

Figure 2: Effects of M on Velocity profiles

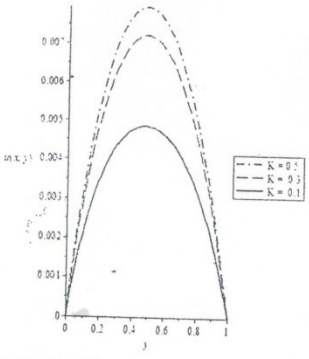

Figure 3: Effects of K on velocity profiles

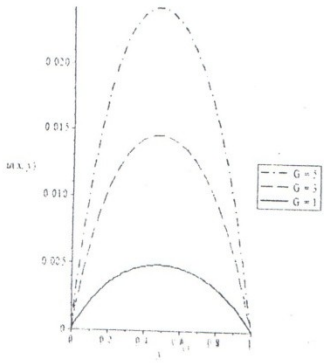

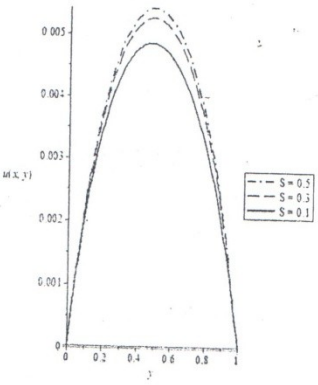

Scientia Africana, Vol. 17 (No. 1), June 2018. Pp 89-102
© Faculty of Science, University of Port Harcourt, Printed in Nigeria *ISSN 1118 – 1931*

Figure 4: Effects of G on Velocity profiles

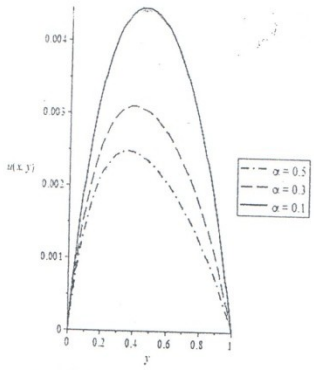

Figure 5: Effects of S on Velocity profiles

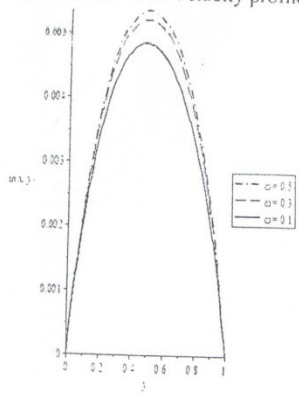

Figure 6: Effects of α on Velocity profiles

Figure 7: Effects of ω on Velocity profiles

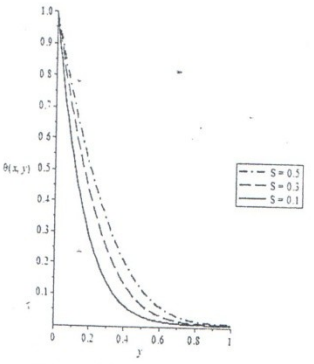

Figure 8: Effects of S on Temperature profiles

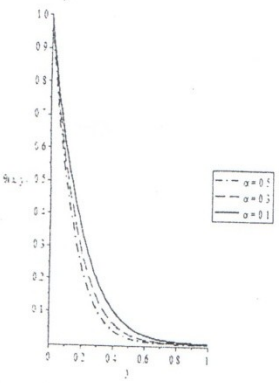

Figure 9: Effects of αon Temperature profiles

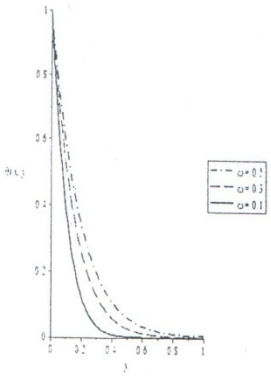

Figure 10: Effects of ω on Temperature profiles

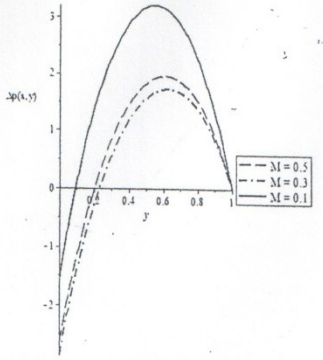

Figure 11: Effects of M on Fluid pressure profiles

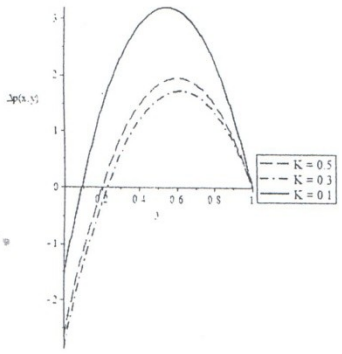

Figure 12: Effects of M on Fluid pressure profiles

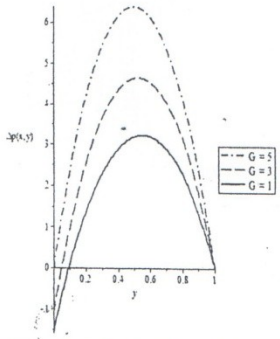

Figure 13: Effects of G on Fluid pressure profiles

Scientia Africana, Vol. 17 (No. 1), June 2018. Pp 89-102
© Faculty of Science, University of Port Harcourt, Printed in Nigeria *ISSN 1118 – 1931*

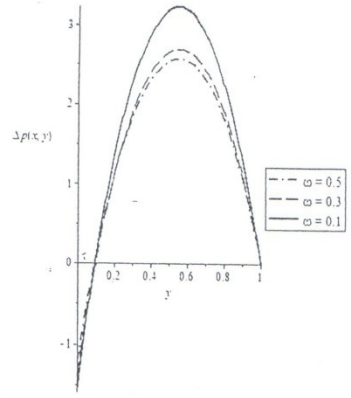

Figure 14: Effects of ω on Fluid pressure profiles

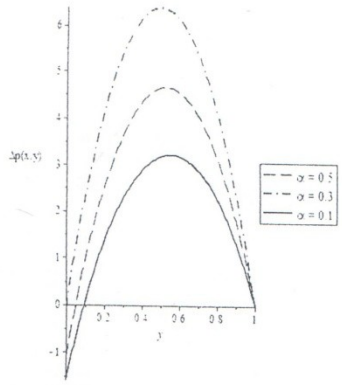

Figure 15: Effects of α on Fluid pressure profiles

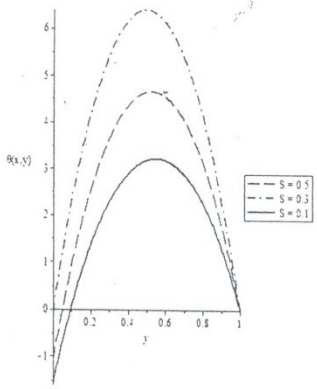

Figure 19: Effects of S on Fluid pressure profiles

The skin friction coefficient and Nusselt number are expressed in equations (68) - (71) are shown in Table 1 and Table 2 for the fluid parameters. The entire fluid parameter take their fixed values expect, the varied parameter. Table 1 shows that increase in value of ω, G, K or S causes a fall in the skin friction while increase in α or M produces a rise in the skin friction coefficient. Table 2 presents that the increase in value ω or S increases the Nusselt number while increase in S reduces the Nusselt number.

Table 1: The skin friction for different values of the fluid parameters

Fluid parameter	Skin friction
$S = 0.1$	-0.1116760
$S = 0.3$	-0.1345073
$S = 0.5$	-0.1507360
M = 0.1	-0.1116760
M = 0.3	-0.1070134
M = 0.5	-0.1042505
K = 0.1	-0.1116760
K = 0.3	-0.1275513
K = 0.5	-0.1322307
G = 0.1	-0.1116760
G = 0.3	-0.1275513
G = 0.5	-0.1322307
$\alpha = 0.1$	-0.1116760
$\alpha = 0.3$	-0.1060528
$\alpha = 0.5$	-0.1012977
$\omega = 0.1$	-0.1116760
$\omega = 0.3$	-0.1060535
$\omega = 0.5$	-0.1012977

Table 2: The Nusselt number for different values of the fluid parameters

Fluid parameter	Nusselt number
$S = 0.1$	4.999996
$S = 0.3$	3.354092
$S = 0.5$	2.687392
$\alpha = 0.1$	4.999996
$\alpha = 0.3$	5.400617
$\alpha = 0.5$	5.777358
$\omega = 0.1$	4.999996
$\omega = 0.3$	5.300647
$\omega = 0.5$	7.773500

The effects of the thermal conductivity on MHD radiative flow in a porous medium between two vertical wavy walls is investigated. The following conclusions were drawn:

i. when the effects of thermal conductivity is taken into account, the flow characteristics changed significantly;

ii. increase in the thermal conductivity parameter (S), radiation parameter (ω), permeability parameter (K) and Grashof number (G) increases the fluid flow while increase in magnetic field parameter (M) and heat source parameter (α) slow down the fluid motion;

iii. temperature of the fluid increases with increase in the thermal conductivity parameter (S) and radiation parameter (ω). But the temperature decreases with the increases with increase in heat source parameter (α);

iv. fluid pressure increases with the increase in values of G, α or S while

Scientia Africana, Vol. 17 (No. 1), June 2018. Pp 89-102
© Faculty of Science, University of Port Harcourt, Printed in Nigeria *ISSN 1118 – 1931*

it decreases with the increase in value of M, K or ω;

v. increase in the value of G, α or S increases the skin friction while increase in M, α or ω reduces in the skin friction; and

vi. increase in the value of α or ω increase the Nusselt number whereas increase in the value of S reduces the Nusselt number.

REFERENCES

Abubakar, J. U. (2014). Natural convective flow and heat transfer in a viscous incompressible fluid with slip effects confined within spirally-enhanced channel. *Unpublished PhD thesis, University of Ilorin.*

Akbar, N. S. (2010) Natural convective MHD peristaltic flow of a nanofluid with convective surface boundary conditions. *J. Compu. Theo. Nana sci, vol 12, no 6, pp257-262.*

Brewster, M.Q. (1972). *Thermal Radiative Transfer Properties, John Wiley 183 and Sons,*

16-25.

Chaim T. C. (1992). Heat transfer in a fluid with variable thermal conductivity over a stretching. *Acta Mech, vol. 95, pp 237- 340.*

Cheng, J., Liao S. J, Mohapatra, R. N and Vajravelu, K. (2008). Series solution of nano boundary layer flows by means of the homotopy analysis method. *Journal of Mathematical Analysis Applications,* 343: 233-245.

Dada, M. S. and Disu, A. B. (2015). Heat transfer with radiation dependent heat source in

MHD free convection flow in a porous medium between two vertical wavy walls. *Journal of the Nigerian Mathematical Society* 34, 200 – 2015.

Disu, A. B. and Dada, M. S. (2017). Reynold's model viscosity on radiative MHD flow in a porous medium between two vertical wavy walls. *Journal of Taibah University for Science* 11 (4), 548 – 565.

Fasogbon, P. F.(2006). MHD ows in corrugated channel. *International Journal of Pure and Applied Mathematics*, 27(2): 225-237.

Fasogbon, P. F.(2010). Analytical studies of heat and mass transfer by convection in a two dimensional irregular channel. *International Journal of Applied Mathematics and Mechanics*, 6(4): 17-37.

Kumar, H. (2011). Heat transfer with radiation and temperature dependent heat source in

MHD free convection flow confined between two vertical wavy walls. *International Journal of Applied Mathematics and Mechanics*, 7(2): 77-103.

Liao S. J.(2004).*Beyond perturbation.A CRC Press Company Boca Raton London New York*
Washington, D.C, 61- 65.

Liao S. J.(2012). *Homotopy analysis method in nonlinear differential equations. Beijind and*
Heidelberg, Springer, 142-146.

Sharma S. A. and Singh S. (2009). Effects of variable thermal conductivity and heat

source/sink on MHD flow near a stagnation point on a linearly sheet. J. Appl. Fluid Mech. Vol. pp. 13-21

Slattery, J. C. (1972). *Momentum energy and Mass transfer in continua. McGraw-Hill. New York*, 32 -37.

Tak, S. S. and Kumar, H. (2006). MHD free convection ow with viscous dissipation in a vertical wavy channel. *Ultra Scientist of Physical Science* 18 (2M): 221-232.

Tak, S. S. and Kumar, H. (2007). Heat transfer with radiation in MHD free convection flow confined between a vertical wavy wall and a wavy at wall. *Bulletin of Pure and Applied Mathematics*, 1(2): 126-140.

Teneja, R. and Jain, N. C.(2004). MHD flow with slip effects and temperature dependent heat source in a viscous incompressible fluid confined between a long vertical wavy wall and a parallel at wall. *Defense Science Journal*, 20(4): 327-340.